Title

Catalytic Cycle of Neisseria meningitidis CMP-Sialic Acid Synthetase Illustrated by High-Resolution Protein Crystallography



Journal

Biochemistry, 59(34)

ISSN

0006-2960

Authors

Matthews, Melissa M
McArthur, John B
Li, Yanhong
et al.

Publication Date

2020-09-01

DOI

10.1021/acs.biochem.9b00517

Peer reviewed

HHS Public Access

Author manuscript

*Biochemistry*. Author manuscript; available in PMC 2021 January 19.

Published in final edited form as:

*Biochemistry*. 2020 September 01; 59(34): 3157–3168. doi:10.1021/acs.biochem.9b00517.

# Catalytic Cycle of *Neisseria meningitidis* CMP-Sialic Acid Synthetase Illustrated by High-Resolution Protein Crystallography

**Melissa M. Matthews**[†,#], **John B. McArthur**[†], **Yanhong Li**[†], **Hai Yu**[†], **Xi Chen**[*,†], **Andrew J. Fisher**[*,†,‡]

[†]Department of Chemistry, University of California, Davis, California 95616, United States

[‡]Department of Molecular and Cellular Biology, University of California, Davis, California 95616, United States

## Abstract

Cytidine 5′-monophosphate (CMP)-sialic acid synthetase (CSS) is an essential enzyme involved in the biosynthesis of carbohydrates and glycoconjugates containing sialic acids, a class of $\alpha$-keto acids that are generally terminal key recognition residues by many proteins that play important biological and pathological roles. The CSS from *Neisseria meningitidis* (NmCSS) has been commonly used with other enzymes such as sialic acid aldolase and/or sialyltransferase in synthesizing a diverse array of compounds containing sialic acid or its naturally occurring and non-natural derivatives. To better understand its catalytic mechanism and substrate promiscuity, four NmCSS crystal structures trapped at various stages of the catalytic cycle with bound substrates, substrate analogues, and products have been obtained and are presented here. These structures suggest a mechanism for an “open” and “closed” conformational transition that occurs as sialic acid binds to the NmCSS/cytidine-5′-triphosphate (CTP) complex. The closed conformation positions critical residues to help facilitate the nucleophilic attack of sialic acid C2-OH to the $\alpha$-phosphate of CTP, which is also aided by two observed divalent cations. Product formation drives the active site opening, promoting the release of products.

## Graphical Abstract

[*]**Corresponding Authors**: xiichen@ucdavis.edu. ajfisher@ucdavis.edu.

[#]**Present Address:** M.M.M.: Molecular Cryo-Electron Microscopy Unit, Okinawa Institute of Science and Technology, Onna-son, Okinawa 904-0495, Japan

Author Contributions

M.M.M., Y.L., H.Y., J.B.M., and A.J.F. performed experiments. All authors analyzed data and wrote the paper. All authors have read and approved the final version of the manuscript.

Supporting Information

The Supporting Information is available free of charge on the ACS Publications website at DOI: 10.1021/acs.biochem.9b00517.

Details of sequence alignments, activation, and inhibition studies and supplemental structure figures (PDF)

The authors declare no competing financial interest.

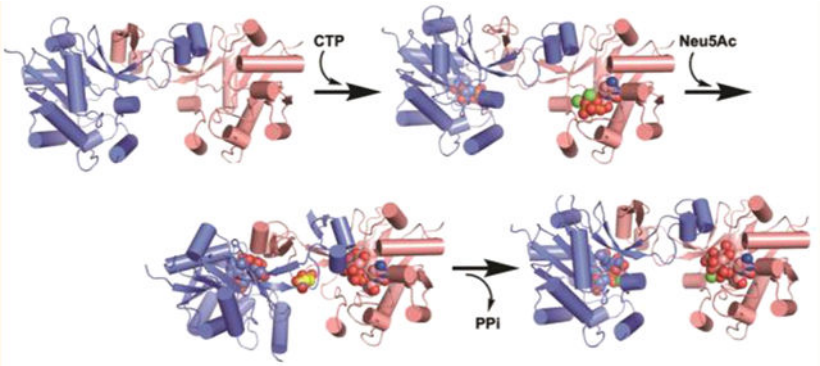


Sialic acid-containing glycoconjugates and oligosaccharides play important roles in human biology and pathology.[1] The key enzymes for the synthesis of these structures are sialyltransferases, which use cytidine-5′-monophosphate-*N*-acetylneuraminic acid (CMP-Neu5Ac), the activated sugar nucleotide, as a donor substrate.[2] CMP-sialic acid synthetases (CSSs)[3,4] catalyze the activation of the β-anomer of the free *N*-acetylneuraminic acid (Neu5Ac) to form a β-linked sialyl monophosphate diester bond between the C-2 of the Neu5Ac and the α-phosphate of the cytidine-5′-triphosphate (CTP) and cleave off pyrophosphate (Scheme 1).

Chemoenzymatic synthetic strategies, which combine chemical synthesis of modified monosaccharides and enzyme-catalyzed activation and transfer of sialic acid and derivatives with or without a sialic acid aldolase-catalyzed reaction, have been proven to be effective strategies for synthesizing sialosides containing natural and non-natural occurring modifications.[5,6] CSSs from different sources have been used together with sialic acid aldolases and/or sialyltransferases for the synthesis of CMP-sialic acids, sialic acid-containing molecules, and their derivatives.[7–12] Comparing to several recombinant bacterial CSSs such as those from *Escherichia coli* K1 (EcCSS),[7,13] *Streptococcus agalactiae* serotype V (SaVCSS),[7,14] *Pasteurella multocida* strain P-1059 (PmCSS), *Hemophillus ducreyi* (HdCSS),[12] and *Clostridium thermocellum* (CtCSS),[15] *Neisseria meningitidis* serogroup B CSS (NmCSS)[7,12] has been proven to be an excellent choice for synthetic applications due to its high expression level (100 mg/L culture), high activity ($k_{cat}/K_m$ = 86 $s^{-1}$ $mM^{-1}$), and promiscuous substrate specificity. It is also active in a broad pH range (7.0–10.0).[7,12] It has been used in the gram-scale synthesis of sialosides[16,17] and has a great potential for industrial scale synthesis. In addition to its native substrate Neu5Ac, NmCSS has been shown to tolerate substrate substitutions at the *N*-acetyl group, C-5, C-7, and C-9.[7,12,18,19] Its toleration toward modifications at C-8,[12,19,20] however, is limited.

Previous structures of NmCSS with and without a cytidine-5′-diphosphate (CDP) inhibitor,[21] mouse CSS catalytic domain,[22] and the homologous *E. coli* cytidine-5′-diphosphate 2-keto-3-deoxy-D-manno-octulosonic acid (CMP-Kdo) synthetase,[23,24] suggest that the enzyme, which exists as a homodimer, rotates about a central dimerization interface upon binding of sialic acid, forming an activated, “closed” state. However, there has been no conclusive evidence for or structures illustrating the proposed closed state. All interactions between sialic acid and the homodimer have only been inferred through mutagenesis-

coupled kinetics experiments,[25] or estimated through docking and modeling software.[21,25,26] Mechanistically, the presence of a conserved DXD motif suggests a role for divalent cations in substrate binding and mechanism. One or two cations have been observed in other CMP-transferases,[23,27] and studies have suggested experimentally that $Mg^{2+}$ is essential for catalysis;[28] however, the precise role and location of $Mg^{2+}$ is unknown. Here four crystal structures of NmCSS are presented including one in the absence of substrate, one with CTP and two calcium ions bound, one with product CMP-Neu5Ac bound, and one with CMP plus a Neu5Ac analogue, 2-deoxy-2,3-dehydro-*N*-acetylneuraminic acid (Neu5Ac2en). These structures provide the molecular framework of NmCSS conformational changes that occur through the catalytic cycle. The discovery of Neu5Ac2en as an NmCSS inhibitor may lead to the development of improved and selective inhibitors against bacterial CSSs as important chemical biological probes and potential therapeutics.

## MATERIALS AND METHODS

### Expression and Purification of $His_6$-Tagged NmCSS.

*Neisseria meningitidis* CMP-sialic acid synthetase (NmCSS) (UniProt Accession ID: P0A0Z8) was expressed and purified as described previously,[7] with the following exceptions: cells were lysed using a microfluidizer instead of lysozyme and DNaseI, and lysate was clarified in a Beckman Avanti J-20 centrifuge using the J-20 rotor at 14 000 rpm for 40 min before loading on the Ni-NTA column. NmCSS can routinely be purified to >95% purity at yields of up to 175 mg/L of cell culture.

### Crystallization of CSS Complexes.

Crystals of the CSS/CMP-sialic acid complex and substrate-free CSS were grown at room temperature by sitting-drop vapor-diffusion. A volume of 1 μL protein solution containing 10 mg/mL of CSS, 8 mM CTP, and 8 mM Neu5Ac was mixed with 1 μL of reservoir (0.16 M calcium acetate, 0.08 M sodium cacodylate pH 6.5, 14.4% PEG 8000, and 20% glycerol). After a month of crystal growth, a single crystal was flash-cooled in liquid nitrogen. The resultant structure revealed that the product, CMP-Neu5Ac, occupied the active site along with a calcium ion in an octahedral coordination geometry. The presence of the product was surprising since it was previously thought that CSS could only use $Mg^{2+}$ to catalyze the formation of a product.[28] Although it is possible that trace $Mg^{2+}$ could have been present in the crystallization buffer, the longer ligand distances between 2.3–2.6 Å of the metal ion suggest that it was calcium instead of magnesium, which has typical ligand distances of ~2.2 Å.[29,30] Presumably when given a month to react during crystal growth, CSS catalyzed the reaction with the nonpreferred cation, $Ca^{2+}$. Eight-month-old crystals from this same drop were soaked in $MgCl_2$ (250 mM) for 30 min to try to replace $Ca^{2+}$ with the preferred $Mg^{2+}$ before flash-cooling in liquid nitrogen. However, rather than yielding the desired Mg-CMP-Neu5Ac structure, diffraction data showed no electron density for any ligand in the active site of these crystals. The crystal structure determined under these conditions is presented here as the ligand-free structure.

Crystals of NmCSS/CTP were grown at room temperature by sitting-drop vapor-diffusion. A volume of 1 μL of protein mixture containing NmCSS (15 mg/mL), CTP (1 mM), and

Neu5Ac (1 mM) was mixed with 1 μL of reservoir (0.1 M imidazole pH 8.0, 6% PEG 8000, and 0.2 M calcium acetate) and allowed to equilibrate. Then 24 h later, rectangular crystals were observed. Assuming that catalysis in the presence of $Ca^{2+}$ would be significantly slower than with $Mg^{2+}$, shortly after crystals were observed, a single crystal was selected and moved into immersion oil prior to flash-cooling in liquid nitrogen. It was anticipated that crystals flash-cooled shortly after nucleation (~24 h), the presence of $Ca^{2+}$ rather than $Mg^{2+}$ might inhibit or slow the enzyme catalysis enough during crystallization to trap a CTP plus Neu5Ac in a "Michaelis-like" complex. However, only electron density for CTP was seen in the active site.

Crystals of NmCSS/CMP/Neu5Ac2en were grown at room temperature using hanging-drop vapor-diffusion. A volume of 200 nL of a protein solution containing NmCSS (15 mg/mL), CTP (1 mM), Neu5Ac2en (10 mM), and $MgCl_2$ (100 mM) was mixed with 200 nL of reservoir (0.1 M sodium citrate/citric acid, pH 5.5, and 20% PEG 3000). After 3 days of equilibration, thick-needle-shaped crystals were observed. A single crystal was selected and transferred to a cryogenic solution containing 30% ethylene glycol before being flash-cooled in liquid nitrogen. This structure resulted in electron density that clearly defines CMP and Neu5Ac2en, suggesting that the presence of $Mg^{2+}$ allowed for the hydrolysis of CTP to CMP, and Neu5Ac2en bound in the active site with CMP.

In an effort to obtain a true precatalytic structure, experiments for cocrystallizing NmCSS with the nonhydrolyzable CTP analogue cytidine-5′-[(α,β)-methyleno]triphosphate (CMPCPP), Neu5Ac, and $Mg^{2+}$ were also attempted. Although crystals diffracted well, no electron density for the analogue was observed in the active site.

### Data Collection, Processing, and Structure Refinement.

Data for the substrate-free crystal were collected on beamline 24-ID-C at the Advanced Photon Source (APS) at Argonne National Laboratory. Data for all protein-substrate complexes were collected on beamline 7–1 at the Stanford Synchrotron Radiation Lightsource (SSRL). All X-ray diffraction data intensities were processed with XDS.[31] Scaling for the ligand-free enzyme-only and NmCSS/CMP-sialic acid complex was done using AIMLESS (CCP4),[32] and scaling for NmCSS/CTP and NmCSS/CMP/Neu5Ac2en was done using the program XSCALE.[31] The previously published NmCSS structure[21] (PDB ID: 1EYR) was used as a model for molecular replacement in CCP4 to solve the phases for all data sets. Data collection and refinement statistics are summarized in Table 1.

The molecular replacement solution for the NmCSS/CMP/Neu5Ac2en structure was initially difficult to interpret because of poor electron density. To resolve this issue, the NmCSS molecular replacement model monomer was broken up into two separate domains. Domain A was made up of residues 1–138 and 170–225 (nucleotide-binding domain), and domain B of residues 139–169 (dimerization domain). The two subunits were used as ensembles in PHASER[33] for an initial round of molecular replacement. The resultant molecular replacement solution had a much improved, interpretable electron density map and revealed more of the closure between the two domains. All models were refined with REFMAC5 (CCP4)[34] and PHENIX.[35]

### Citrate Activation Assay.

A 20 μL reaction mixture containing NmCSS (20 ng), $MgCl_2$ (10 mM), Tris-HCl (100 mM, pH 8.5), CTP (1 mM), Neu5Ac (1 mM), and sodium citrate (0, 1, 5, 10, or 20 mM) was incubated at 37 °C in duplicate for 10 min. The reaction was stopped with 20 μL of precooled ethanol and analyzed by capillary electrophoresis according to a previously reported protocol.[12] The experiment was repeated on a separate day, and all percent conversion values were averaged for each concentration of citrate.

### NmCSS Mutagenesis and Activity Assays.

NmCSS mutants E162A [(forward primer) 5′-GCCCAGCCTCGCCAACAATTACC-3′ and (reverse primer) 5′-CAAATCGCTTAGATGGCGCATGGG-3′], E162Q [(forward primer) 5′-CAGCAGCCTCGCCAACAATTACCTCAGG-3′ and the reverse primer was the same as that for the E162A mutant)], and R165A [(forward primer) 5-GCCCAACAATTACCTCAGGCATTTAGGC-3′ and (reverse primer) 5′AGGCTGCTCCAAATCGCTTAGATGG-3′)] were prepared by Q5 site-directed mutagenesis, expressed in 50 mL cultures, and purified by Ni-NTA chromatography. For assays, a 40 μL reaction mixture containing NmCSS (4 ng) or its mutant (50 ng of E162A or E162Q, or 5 μg of R165A), $MgCl_2$ (10 mM), Tris-HCl (100 mM, pH 8.5), CTP (3 mM), and Neu5Ac (1 mM) was incubated at 37 °C in duplicate for 30 min. The reaction was stopped with 40 μL of precooled methanol and quantified with an Infinity 1290-II HPLC equipped with a UV-vis detector (Agilent Technologies, CA) and a CarboPac PA100 anion exchange column (Dionex), using a gradient from 0% to 90% 2 M ammonium acetate, pH 6.0, over 10 min against water.

### Neu5Ac2en and Calcium Chloride Inhibition Assays.

For Neu5Ac2en and calcium chloride inhibition assays, reactions were carried out at 37 °C for 30 min in 40 μL reaction mixtures containing CTP (3 mM), Neu5Ac (2 mM), NmCSS (8 ng), $MgCl_2$ (10 mM), and Tris-HCl buffer (100 mM, pH 8.5) with or without Neu5Ac2en (0, 0.01, 0.02, 0.05, 0.1, 0.2, 0.5, 1, 2, 5, 10 mM) or $CaCl_2$ (0, 5, 10, 20, 50, or 100 mM). The reactions were quenched and analyzed similarly to that described for the mutant assays. Data were analyzed using Grafit 5.0.

## RESULTS

### Overall Structure.

The ligand-free structure crystallizes with one monomer in the asymmetric unit with the crystallographic 2-fold generating the biologically functional dimer. The ligand-free structure presented here has an improved resolution (1.75 Å) compared to the formerly published NmCSS ligand-free structure (2.00 Å) (PDB ID: 1EZI).[21] The two structures superimpose with a 0.70 Å RMSD for all 216 modeled equivalent α-carbons. NmCSS exists as a homodimer where each monomer is composed of a globular nucleotide-binding domain and an extended dimerization domain (Figure 1A). The dimerization domain comprises a ~35 residue insert corresponding to residues 136–171 and “domain-swaps” with the dimerization domain of the related crystallographic monomer to generate a tightly entwined

complex. Improved resolution and more favorable crystal contacts allowed us to resolve the structure of the loop between αD and αE (residues 71–80), which was disordered in the previously published ligand-free structure (PDB ID: 1EZI).[21] The carbon backbone of the P-loop (residues 12–22) (Figure S1) was visible in the electron density, but the side-chain density for Lys16 was poor and was modeled as an alanine stub. The average B-value for this region remains high at 68.7 $Å^2$, compared to an average B-value of 28.5 $Å^2$ for the entire structure.

### Structure of the NmCSS Calcium-CTP Complex.

The NmCSS calcium-CTP complex crystallized with a dimer in the asymmetric unit, and the structure was determined to 1.8 Å resolution. Many residues involved in nucleotide binding were elucidated in the NmCSS–CDP structure published previously (PDB ID: 1EYR).[21] However, the NmCSS–CDP structure revealed two conformations of the diphosphate moiety of CDP, resulting in the ambiguity of understanding how Mg-CTP binds and the relative orientation and interactions between substrates Mg-CTP and Neu5Ac. The structure reported here clearly shows CTP with two $Ca^{2+}$ ions binding in the active site of monomer A with the conformation of the triphosphate moiety pointing in a similar direction to Conformation I in the previously published CDP structure[21] (Figure 2). Our CTP-bound structure also reveals that monomer B binds a CTP molecule without calcium ligands, resulting in a slightly different conformation for the triphosphate moiety. This difference highlights the effect of divalent cations in the positioning of CTP (Figure S2). However, the electron density for the β- and γ-phosphates is weak, suggesting partial CTP hydrolysis in the B subunit. Nevertheless, for the A subunit, two calcium ions are observed to bind to the CTP triphosphate (Figure 2). The triphosphate group wraps around $Ca^{2+}$(B), allowing the β-phosphate to form a hydrogen bond with Ser15 and the β- and γ-phosphate to interact with Arg12 of the P-loop. This triphosphate conformation binding to $Ca^{2+}$(B) exposes the backside of the α-phosphate to solvent or a potential sialic acid that would bind in the active site. However, in the absence of $Ca^{2+}$ in the B subunit, the triphosphate group adopts a staggered conformation with no interaction between the β-phosphate and Ser15 or Arg12. As a result, the side of the α-phosphate, which should be exposed, is pointed back toward the ribose moiety and is less accessible to a nucleophilic attack. Unless otherwise noted, all further discussion of the NmCSS/CTP structure refers strictly to the CTP/$Ca^{2+}$/$Ca^{2+}$ complex, focusing on the A subunit.

Binding of CTP/$Ca^{2+}$/$Ca^{2+}$ stabilizes the P-loop, as evidenced by its lower average B-value (18.9 $Å^2$) and clear electron density as compared to that of the ligand-free structure, including defining the conformation of Lys16. The highly conserved, positively charged P-loop residues Arg12 and Lys21 (Figure S1) ion-pair with the negatively charged triphosphate group of CTP (Figure 2). Electrostatic interactions are present between Lys21 and the α-phosphate group as well as between Arg12 and the β- and γ-phosphates. Ser15 hydrogen-bonds with the β-phosphate, and the backbone amino groups of both Lys16 and Gly17 fix the proper positioning of the γ-phosphate through hydrogen-bonding interactions (Figure 2). The amide group of Asn22 in the P-loop makes two hydrogen bonds to the 2′- and 3′-OH of the ribose sugar.

The CTP/$Ca^{2+}$/$Ca^{2+}$ binding pocket P-loop is also stabilized by an interaction between conserved Lys16 and conserved Asp78, which in turn interacts with Arg12 (Figure 2). This interaction helps to position the loop (residues 71–80) that binds to and selects for cytidine base of the nucleotide, where Arg71 donates two hydrogen bonds to O2 and N3 of cytidine, and the main chain carbonyl of Ala80 accepts a hydrogen bond from N4 (Figure 2).

The two calcium ions in the NmCSS/CTP structure, denoted $Ca^{2+}$(A) and $Ca^{2+}$(B), each play different but important roles in the chemistry of binding and catalysis. $Ca^{2+}$(B) interacts more directly with the triphosphate group, binding to all three phosphates in the pentagonal bipyramidal primary coordination sphere. Meanwhile, $Ca^{2+}$(A) coordinates only the $\alpha$-phosphate directly. Conserved Asp209 and Asp211, of the DXD sequence, position $Ca^{2+}$(A) through both direct coordination (Asp211) and indirect coordination (Asp209) via $Ca^{2+}$(A)-bound waters. (Figure 2) This finding supports previous activity studies of the poorly functioning D209A and D211A NmCSS mutants.[25] These studies showed that, while the D209A and D211A mutations are both detrimental to enzyme function, increased concentrations of $Mg^{2+}$ increases the reaction rate of D211A two times more than it increases the reaction rate for D209A. This is consistent with the structure that demonstrates Asp211 directly coordinates the divalent metal ion, but Asp209 interacts with the metal ion water ligands. Sequence conservation also suggests a less direct role for Asp209, because it is glutamate in some species, including Drosophila (Supplemental Figure S1).

Divalent cations are strictly required for catalytic activity.[4,25] While the majority of CSS enzymes require $Mg^{2+}$ or $Mn^{2+}$, most are either inhibited or display greatly diminished activity with $Ca^{2+}$.[4] We also confirmed that $Ca^{2+}$ inhibits NmCSS with an $IC_{50}$ value of 8.8 ± 0.4 mM (Figure S3). However, given that $Ca^{2+}$ coordination is very similar to $Mg^{2+}$ coordination geometries, this CTP/$Ca^{2+}$/$Ca^{2+}$ complex structure reported here is an ideal Michaelis complex analogue of the first substrate binding in this ordered Bi–Bi catalytic mechanism. Furthermore, the CTP-$Ca^{2+}$(B) substrate complex here is very similar to the CTP-$Mg^{2+}$ complex observed in *E. coli* CMP-Kdo synthetase,[23] where the $Mg^{2+}$ ion is coordinated by all three phosphates of CTP. Unfortunately, this CMP-Kdo synthetase structure did not observe the second $Mg^{2+}$ ion binding site but speculated it would bind in a similar location to the $Ca^{2+}$(A) ion reported here.[23] However, a $Mg^{2+}$ ion was observed in another CMP-Kdo synthetase structure in a similar location to the $Ca^{2+}$(A) ion.[24]

## Binding of Sialic Acid Induces Active Site Closing.

Conformational changes are seen in the active site of *E. coli* CMP-Kdo-forming enzyme upon binding of an analogue of 2-keto-3-deoxymanno-octulonic acid (Kdo),[23,24] leading us to hypothesize a similarly closed conformation my occur in NmCSS. To successfully capture this state, 2-deoxy-2,3-dehydro-*N*-acetylneuraminic acid (Neu5Ac2en) was utilized. Neu5Ac2en is a dehydrated sialic acid analogue that lacks the attacking C2-OH group responsible for the formation of CMP-sialic acid and having a double bond between C2 and C3 instead. In the absence of this hydroxyl group, Neu5Ac2en can bind in the active site pocket with CTP but traps the enzyme in an intermediate state that parallels the enzyme structural state before catalysis occurs. Inhibition studies confirmed that Neu5Ac2en was an inhibitor with an $IC_{50}$ value of 0.13 ± 0.01 mM under the assay conditions used (Figure S4).

Neu5Ac2en was successfully trapped in the NmCSS active site; however, the structure revealed that during crystallization, the enzyme hydrolyzed CTP to CMP and CMP was observed bound in the active site with bound Neu5Ac2en (Figure 1B). Nevertheless, the crystal structure of this ternary complex revealed the enzyme in a more closed state, relative to ligand-free and Ca/CTP bound structures (Figure 1B and Figure 3).

The closed state of NmCSS/CMP/Neu5Ac2en is brought about by rotation about pivot points located at the termini of $\beta$-strands 5 and 8 at the base of the dimerization domain. The flexible nature of the residues at this location at the boundary of the nucleotide-binding and dimerization domain, including conserved Ser132, Ala133, and Gly176, enables active site closure without enacting large conformational change in the individual domains. The nucleotide-binding domain (residues 1–134 and 175–224) of the CTP-bound and the CMP/Neu5Ac2en-bound conformations superimpose with an RMSD of only 0.430 Å for all modeled equivalent $\alpha$ carbons. At the same time, the dimerization domain (residues 135–174) of the CTP-bound and the CMP/Neu5Ac2en-bound conformations superimpose with an RMSD of only 0.658 Å for all modeled equivalent $\alpha$ carbons. While the domains themselves remain rigid, the angle between them changes significantly, moving NmCSS into the closed conformation resulting in the dimerization domain of one subunit closing in on the active site of the other subunit in the dimer. In the CMP/Neu5Ac2en-bound structure, the dimerization domain has rotated so that the $\beta$5/$\beta$6 loop and $3_{10}$ helix cover most of the exposed surface of the occupied active site, closing off the active site from bulk solvent (Figure 3).

Active site closing is initiated through interactions between the sialic acid analogue and the dimerization domain of the other monomer, monomer B (Figure 3B and Figures 4A,B). Lys142 of monomer B, located at the end of the dimerization domain's $3_{10}$ helix, and the backbone nitrogen of Arg165, reach into the active site of monomer A to interact with Neu5Ac2en's carboxylate group. Lys142 and the Leu161 backbone carbonyl each form a hydrogen bond with the C7-OH. The Glu162 backbone carbonyl oxygen hydrogen-bonds with C4-OH. After the initial closing, which involved interactions between protein and sialic acid, the closed conformation is stabilized by several intermonomer interactions. Gln166(B) of the $3_{10}$ helix bridges the gap between monomers through hydrogen bonding with the backbone carbonyl of Asp78(A) (Figure 3B). His138(B) and Arg173(A) interact via $\pi$–$\pi$-stacking and His138(B) also forms a salt bridge with Asp209(A).

In addition to the interactions with the dimerization domain of the opposite monomer, sialic acid also interacts with several highly or partially conserved residues (Figure S1) in the nucleotide-binding domain. The methyl group in the *N*-acetyl of Neu5Ac2en lies in a hydrophobic pocket made up of Leu102, Tyr179, and Phe192. Additionally, The N$\varepsilon$2 of Gln104 hydrogen-bonds with O8 of Neu5Ac2en. The Ser82 backbone nitrogen hydrogen-bonds to O4 of Neu5Ac2en while its O$\gamma$ hydrogen-bonds with the *N*-acetyl nitrogen (Figure 4A,B).

In spite of having $Mg^{2+}$ present in crystallization solution, no cations are observed in the active site of the NmCSS/CMP/Neu5Ac2en structure. This is most likely due to the absence

of the cytidine nucleotide's β- and γ-phosphates, which were hydrolyzed during the course of the crystallography experiment.

### Enzyme Activation by Citrate?

Unaccountable electron density was observed at the dimer interface in the NmCSS/CMP/Neu5Ac2en structure. Given the crystals were grown in the presence of citrate (100 mM), a citrate molecule was modeled in which fits the electron density acceptably (Figure S5A). This citrate molecule bridges the gap between the two dimerization domains and also forms a conduit between the one dimerization domain and the nucleotide-binding domain of the opposite monomer (Figure S5A). Citrate's two terminal carboxylate groups reach across the space between the two monomers at their β5/β6 loop, hydrogen-bonding with the backbone nitrogens of the Glu137 in each. The citrate also connects two side chains from opposite monomers, the central carboxylate interacting with the Nδ1 of His138 and the one of the terminal carboxylates interacting with the Nε2 of His204.

Considering the importance of the β5/β6 loop in enzyme closing and the role of His138 in stabilizing the NmCSS closed conformation, we hypothesized that citrate may affect CSS activity. Indeed, after adding citrate to the reaction buffer, the production of CMP-sialic acid was increased moderately (Figure S5B). Further work will be necessary to determine the precise role of citrate in the regulation of CSS activity.

### Structure with the CMP-Neu5Ac Product Bound.

The crystal structure of NmCSS with CMP-Neu5Ac product bound revealed a structure in the open state conformation similar to the ligand-free and Ca-CTP bound state of NmCSS. This suggests that after binding CTP and Neu5Ac, product formation drives the reopening of the active site, possibly to release products. Sialic acid interactions with the nucleotide-binding domain are maintained, but as a new bond is formed between the sialic acid and the α-phosphate, the sugar group moves deeper into the active site pocket of the nucleotide-binding domain breaking interactions between the sugar and dimerization domain, and NmCSS transitions back into an open state. At this point, $Ca^{2+}$(B) leaves the active site with the pyrophosphate, but $Ca^{2+}$(A) remains, coordinating the Neu5Ac carboxylate group, an oxygen in the phosphate moiety of CMP-Neu5Ac, and four ordered water molecules in an octahedral geometry (Figure 5). The ordered waters are also held in place with the help of the metal-binding DXD motif of Asp209 and Asp211. The DXD-containing loop is nudged open a small amount so Asp211 no longer coordinates $Ca^{2+}$(A) directly as observed in the Ca-CTP bound structure.

### Comparison with Other Structures.

With less than 30% sequence identity to NmCSS, the crystal structures of *E. coli* CMP-Kdo synthetases KdsB[23] and KpsU[24] as well as mouse CSS (MmCSS)[22] have parallels as well as differences with the structures presented here. Although several residues are highly conserved (Figure S1), the process and means of closed state formation varies from species to species.

While the *E. coli* CMP-Kdo synthetases are active dimers, they do not possess dimerization domains that entwine and lock the two monomers together as observed in NmCSS. This flatter dimerization interface only buries 2673 $Å^2$ of surface area of both monomers in the closed state compared to NmCSS closed state, which buries 4460 $Å^2$. However, the *E. coli* structures also display a conformational change that closes the active site pocket in the presence of two substrates, but not after product formation, reminiscent of what we observe in NmCSS.

While we were unable to capture the NmCSS/CTP/sialic acid structure, the KdsB/CTP/2-keto-2,3-deoxymanno-octulonic acid (Kdo2en) structure indicates that the guanidinium group of Arg164 (Arg165 in NmCSS) is involved in CTP $\gamma$-phosphate interaction (Figures 6A,B). Superposition of the NmCSS/CTP and NmCSS/CMP/Neu5Ac2en structures suggests a similar function for Arg165 in NmCSS (Figure 6A). Because the *E. coli* CMP-Kdo synthetases form different dimerization interactions and lack the dimerization domain, no residues of one monomer contact the sugar bound in the active site of the partner monomer. However, Glu210 of the nucleotide-binding domain of KdsB hydrogen bonds with C4-OH of the Kdo analogue through its carboxylate group and backbone nitrogen (Figure 6B). Structurally, KdsB Glu210 is in the same position as Glu162 of NmCSS; however, in KdsB, Glu210 is from the same monomer as the active site in which Kdo2en is situated, but in NmCSS Glu162 is from the dimerization domain of the opposite monomer. KdsB Arg157, which ion-pairs with Kdo2en carboxylate group in a position similar to that of CSS Lys142, is also from the same monomer.

The dimerization domain of mouse CSS, which is similar to NmCSS, does interact with the sugar in the opposite monomer's active site through two arginine residues. Similar to Arg165 of NmCSS, the Arg202 backbone amino group of MmCSS binds to the Neu5Ac carboxylate group. Interestingly, in MmCSS the arginine guanidinium group ion-pairs with the Neu5Ac carboxylate group as well, giving the Arg202 side chain a role in closed-state stabilization. The R202A mutation has been shown to be detrimental but not fatal to enzyme activity, while the NmCSS R165A mutation results in a complete loss of activity.[36] The ability of MmCSS to function without Arg202 may be due to additional closed-state stabilization from MmCSS Arg199, which hydrogen bonds with both the Neu5Ac C7 hydroxyl and the *N*-acetyl carbonyl group (Figure 6C). The position of Arg199 allows it to also form three new interactions with Glu211 and Gln229 of the partner monomer (Figure 6C). Due to this extra closed-state stabilization, MmCSS remains closed even after product formation. NmCSS Arg165, however, may play a different role in directing NmCSS enzyme–substrate conformation, as we discuss below.

### Modeling of CSS/CTP/$Ca^{2+}$/$Ca^{2+}$/Neu5Ac.

Arg165 is strictly conserved in both CMP-sialic acid and CMP-Kdo synthetases (Figure S1), yet there are no explicit interactions between Arg165 side-chain atoms and Neu5Ac2en or CMP in the NmCSS/CMP/Neu5Ac2en structure. A superposition of CTP from the NmCSS/CTP structure onto the NmCSS/CMP/Neu5Ac2en structure indicates that Arg165(B) could form electrostatic interactions with the $\gamma$-phosphate of CTP (Figure 6A), which would corroborate with the function of its equivalent residue in KdsB. The side-chain

electron density for Arg165 in NmCSS/CMP/Neu5Ac2en is weak, and the position shown in Figure 6A would not be possible in the presence of $Ca^{2+}$(A). However, since the structure is missing the complete triphosphate moiety, it cannot be regarded as a true intermediate state of the NmCSS catalytic cycle. An alternative Arg165 rotamer has been modeled which maintains the ion pair between Arg165 and the $\gamma$-phosphate but does not clash with $Ca^{2+}$(A) (Figure 7A).

Since Arg165 is a long, positively charged residue capable of reaching across the gap between the dimerization and nucleotide-binding domains, the highly conserved nature of Arg165 may be due to the need for proper positioning of the backbone of residue 165. Perhaps the anchoring of Arg165 with the $\gamma$-phosphate is necessary in order to allow its backbone amino group to interact with the Neu5Ac carboxylate group.

### Activity of NmCSS Mutants.

The four crystal structures presented above led us to hypothesize the functional role of two key residues in helping to stabilize the closing of the active site, making them important in the catalytic mechanism proposed below. Specifically, it appears that Glu162 and Arg165 may play an important role by reaching across the dimer interface to possibly interact with substrates in the other monomer's active site. Glu162 and Arg165 interact with the sialic acid and the triphosphate moiety from CTP, respectively, in the other subunit's active site (Figure 3B). Glu162 also stabilizes the active-site closure by hydrogen bonding with the mainchain nitrogen of Phe192 in the other monomer.

Indeed, the E162A and E162Q mutants displayed 6-fold lower activity than the wild-type NmCSS, while the R165A mutant was approximately six hundred-fold less active than wild-type (Table 2). These results suggest that the active-site closure, stabilized by cross-monomer interactions involving residues Glu162 and Arg165, is necessary for efficient catalysis.

## DISCUSSION

### Basis for Substrate Tolerance.

In the chemoenzymatic synthesis of complex carbohydrates, NmCSS has proven itself to be a very useful enzyme, activating several forms of sialic acids as diverse as 2-keto-3-deoxy-D-manno-octulosonic acid (Kdo) and *N*-azidoacetylneuraminic acid ($Neu5AcN_3$). The structures presented here enable us to better understand the basis of this tolerance. First off, the flexible nature of the Lys142 side chain would likely allow for substitutions at O7 as well as small changes in the position of the Neu5Ac carboxylate group. Additionally, analysis of the active site pocket after closing suggests that a solvent pocket near C7, C8, and C9 provides space for bulky modifications to O9 (Figure 4A). It could also provide space for sialic acid to shift deeper into the active site pocket in order to allow *N*-acetyl modification as well. In fact, these are the modifications that are tolerated by the enzyme.[7,12,19] Modification of the C8 hydroxyl group, however, results in a drastic decrease in activity.[12] In light of the structures presented here, this is likely due to the importance of the Gln104–O8 interaction in the initial docking of sialic acid.

Although few crystal structures of NmCSS have been available previously, several groups have successfully created mutants of NmCSS with increased or modified substrate specificity. The S81R mutant of NmCSS, for example, has been shown to better tolerate O8-methyl substitutions.[26] Model-guided mutagenesis has also created mutants that have more general tolerance for *N*-acyl-modified sialic acids.[26] Despite these success stories, however, there is still a need for mutants that can accept substrates with more than one modification such as Neu5Gc8OMe or Kdo8OMe. Based on the NmCSS/CMP/Neu5Ac2en and NmCSS/CMP-Neu5Ac structures presented here, shortening or mutating the loop between $\beta$-sheet 8 and 9 may allow more room for C8 modifications as well as provide more space for small shifts of sialic acid due to multiple modifications.

## Role of $Mg^{2+}$ in Catalysis.

Previous studies have suggested that only $Mg^{2+}$ can be used by NmCSS to catalyze nucleotide transfer to sialic acid.[28] Since the product was formed over a month's time in the crystallization drop with $Ca^{2+}$ rather than $Mg^{2+}$, clearly the identity of the cation is not strictly limited to $Mg^{2+}$, but catalysis using $Ca^{2+}$ may be much slower than with $Mg^{2+}$. In fact, calcium has been reported to substitute for $Mg^{2+}$ in other CSS enzymes, although usually with less catalytic efficiency.[37–39] Figure 2 and Figure S2 demonstrate the important role of divalent cations in the proper positioning of the triphosphate groups. Divalent metal $M^{2+}$(B) coordinates all three phosphate groups and orients the scissile bond between the $\alpha$-phosphate and $\beta$-phosphate to be along the same axis as the attack by Neu5Ac on the $\alpha$-phosphate. $M^{2+}$(B) also increases the leaving group potential of the pyrophosphate moiety by stabilizing its negative charge. Even with proper orientation and the presence of a good leaving group, however, the C2-OH of Neu5Ac must first be deprotonated before it can attack the $\alpha$-phosphate, and there is no basic residue within close enough proximity to play this role. $M^{2+}$(A) likely solves this problem by decreasing the p$K_a$ of the hydroxyl group by ligating directly to the $M^{2+}$(A) ion. We propose that both the anomeric C2-OH and the C1-carboxylate group of Neu5Ac directly ligate to $M^{2+}$(A), which positions the anomeric C2 hydroxyl group in prime position for a nucleophilic attack on the $\alpha$-phosphate. This model is corroborated by the NmCSS/CMP-Neu5Ac structure that has the Neu5Ac carboxylate group ligated to $Ca^{2+}$(A) after catalysis. Hydroxyl activation via $Mg^{2+}$ coordination has also been proposed for the catalysis of KdsB,[23] which uses the metal to activate 2-keto-3-deoxymanno-octulonic acid (Kdo). Based on structural analysis and EPR data,[23,27] the locations of the $Mg^{2+}$ in both EcKdsB and AaKdsB have been elucidated. Overlay of AaKdsB with the NmCSS/CTP/Ca/Ca structure shows that the metal positions in these structures are similar, supporting a similar mechanism as well.

## Proposed Catalytic Cycle for NmCSS.

Careful analysis of each structure presented here allows us to hypothesize an enzyme conformation for each step in the catalytic cycle of NmCSS catalysis (Figure 7B). At the start of the catalytic cycle, CTP binds in the active site pocket along with $M^{2+}$(A) and $M^{2+}$(B), which properly position the phosphate groups for catalysis and allow space for Neu5Ac to enter the active site pocket. Arg12 moves to interact with the $\beta$- and $\gamma$-phosphates. With CTP in this position, Neu5Ac loosely binds in the available space in the active site of monomer A, with its carboxylate group and the anomeric carbon hydroxyl group in the

coordination shell of $M^{2+}$(A). The binding of Neu5Ac initiates active site closure as the interactions between sialic acid and Lys142, Leu161, Glu162, and Arg165 pull sialic acid, CTP, and the nucleotide-binding domain toward the dimerization domain (Figure 3). Once initiated, the closed state is stabilized by Arg165 ion pairing with the $\gamma$-phosphate and several intermonomer interactions. As the dimerization domain comes near to Neu5Ac, coordination to $M^{2+}$(A) allows Neu5Ac–C2–OH to be deprotonated, with the proton possibly being shuttled through water ligands to Asp209. The restricted movement by the presence of the dimerization domain forces the deprotonated oxygen toward CTP's $\alpha$-phosphate, which has an increased electrophilic nature due to the two $M^{2+}$'s that coordinate the triphosphate group and the Arg165 to $\gamma$-phosphate ion pair. As the bond between the $\alpha$-phosphate and $\beta$-phosphate breaks and the new bond between Neu5Ac–O2 and $\alpha$-phosphate forms, the $\alpha$-phosphate passes through a trigonal bipyramidal transition state, and pyrophosphate and its associated $M^{2+}$(B) leave the active site. Once the product has been formed, the sugar is more closely associated with the nucleotide-binding domain and can no longer maintain its hydrogen bonding and electrostatic interactions with the dimerization domain, so NmCSS/CMP-Neu5Ac reverts back to the open state. The product diffuses from the active site, and the cycle can begin again.

Although NmCSS has been used in chemoenzymatic synthesis of sialic acid-containing structures for over a decade, the causes for its broad substrate tolerance and the role of divalent cations in catalysis have finally been shown through the four structures presented here. This work describes how sugar interaction with both monomers of the NmCSS homodimer are responsible for active site closure and the role of divalent cations in the transfer of CMP to sialic acid, laying the groundwork for future structure-guided enzyme engineering.

## Supplementary Material

Refer to Web version on PubMed Central for supplementary material.

## ACKNOWLEDGMENTS

This work is based upon research conducted at the Northeastern Collaborative Access Team beamlines, which are funded by the National Institute of General Medical Sciences from the National Institutes of Health (P30 GM124165). The Pilatus 6 M detector on 24-ID-C beamline is funded by an NIH-ORIP HEI grant (S10 RR029205). This research used resources of the Advanced Photon Source, a U.S. Department of Energy (DOE) Office of Science User Facility operated for the DOE Office of Science by Argonne National Laboratory under contract no. DE-AC02-06CH11357. Use of the Stanford Synchrotron Radiation Lightsource, SLAC National Accelerator Laboratory, is supported by the U.S. Department of Energy, Office of Science, Office of Basic Energy Sciences under contract no. DE-AC02-76SF00515. The SSRL Structural Molecular Biology Program is supported by the DOE Office of Biological and Environmental Research and by the National Institutes of Health, National Institute of General Medical Sciences (including P41GM103393). The contents of this publication are solely the responsibility of the authors and do not necessarily represent the official views of NIGMS or NIH.

Funding

This work was partially supported by the United States National Institutes of Health (NIH) grants (U01GM120419, U01GM125288, and R01AI130684). The content is solely the responsibility of the authors and does not necessarily represent the official views of the National Institutes of Health.

## REFERENCES


(1). Varki A (2008) Sialic acids in human health and disease. Trends Mol. Med 14, 351–360. [PubMed: 18606570]

(2). Li Y, and Chen X (2012) Sialic acid metabolism and sialyltransferases: natural functions and applications. Appl. Microbiol. Biotechnol 94, 887–905. [PubMed: 22526796]

(3). Sellmeier M, Weinhold B, and Munster-Kuhnel A (2013) CMP-Sialic Acid Synthetase: The Point of Constriction in the Sialylation Pathway. Top. Curr. Chem 366, 139–167.

(4). Mizanur RM, and Pohl NL (2008) Bacterial CMP-sialic acid synthetases: production, properties, and applications. Appl. Microbiol. Biotechnol 80, 757–765. [PubMed: 18716769]

(5). Chen X, and Varki A (2010) Advances in the biology and chemistry of sialic acids. ACS Chem. Biol 5, 163–176. [PubMed: 20020717]

(6). Li W, McArthur JB, and Chen X (2019) Strategies for chemoenzymatic synthesis of carbohydrates. Carbohydr. Res 472, 86–97. [PubMed: 30529493]

(7). Yu H, Yu H, Karpel R, and Chen X (2004) Chemoenzymatic synthesis of CMP-sialic acid derivatives by a one-pot two-enzyme system: comparison of substrate flexibility of three microbial CMP-sialic acid synthetases. Bioorg. Med. Chem 12, 6427–6435. [PubMed: 15556760]

(8). Chokhawala HA, Yu H, and Chen X (2007) High-throughput substrate specificity studies of sialidases by using chemoenzymatically synthesized sialoside libraries. ChemBioChem 8, 194–201. [PubMed: 17195254]

(9). Yu H, Huang S, Chokhawala H, Sun M, Zheng H, and Chen X (2006) Highly efficient chemoenzymatic synthesis of naturally occurring and non-natural $\alpha$−2,6-linked sialosides: a P. damsela $\alpha$−2,6-sialyltransferase with extremely flexible donor-substrate specificity. Angew. Chem., Int. Ed 45, 3938–3944.

(10). Yu H, Chokhawala H, Karpel R, Yu H, Wu B, Zhang J, Zhang Y, Jia Q, and Chen X (2005) A multifunctional Pasteurella multocida sialyltransferase: a powerful tool for the synthesis of sialoside libraries. J. Am. Chem. Soc 127, 17618–17619. [PubMed: 16351087]

(11). Yu H, Cheng J, Ding L, Khedri Z, Chen Y, Chin S, Lau K, Tiwari VK, and Chen X (2009) Chemoenzymatic synthesis of GD3 oligosaccharides and other disialyl glycans containing natural and non-natural sialic acids. J. Am. Chem. Soc 131, 18467–18477. [PubMed: 19947630]

(12). Li Y, Yu H, Cao H, Muthana S, and Chen X (2012) Pasteurella multocida CMP-sialic acid synthetase and mutants of Neisseria meningitidis CMP-sialic acid synthetase with improved substrate promiscuity. Appl. Microbiol. Biotechnol 93, 2411–2423. [PubMed: 21968653]

(13). Liu G, Jin C, and Jin C (2004) CMP-N-acetylneuraminic acid synthetase from Escherichia coli K1 is a bifunctional enzyme: identification of minimal catalytic domain for synthetase activity and novel functional domain for platelet-activating factor acetylhydrolase activity. J. Biol. Chem 279, 17738–17749. [PubMed: 14960566]

(14). Yu H, Ryan W, Yu H, and Chen X (2006) Characterization of a bifunctional cytidine 5′-monophosphate N-acetylneuraminic acid synthetase cloned from Streptococcus agalactiae. Biotechnol. Lett 28, 107–113. [PubMed: 16369694]

(15). Mizanur RM, and Pohl NL (2007) Cloning and characterization of a heat-stable CMP-N-acylneuraminic acid synthetase from Clostridium thermocellum. Appl. Microbiol. Biotechnol 76, 827–834. [PubMed: 17602221]

(16). Yu H, Santra A, Li Y, McArthur JB, Ghosh T, Yang X, Wang PG, and Chen X (2018) Streamlined chemoenzymatic total synthesis of prioritized ganglioside cancer antigens. Org. Biomol. Chem 16, 4076–4080. [PubMed: 29789847]

(17). Yu H, Yan X, Autran CA, Li Y, Etzold S, Latasiewicz J, Robertson BM, Li J, Bode L, and Chen X (2017) Enzymatic and Chemoenzymatic Syntheses of Disialyl Glycans and Their Necrotizing Enterocolitis Preventing Effects. J. Org. Chem 82, 13152–13160. [PubMed: 29124935]

(18). Khedri Z, Li Y, Muthana S, Muthana MM, Hsiao CW, Yu H, and Chen X (2014) Chemoenzymatic synthesis of sialosides containing C7-modified sialic acids and their application in sialidase substrate specificity studies. Carbohydr. Res 389, 100–111. [PubMed: 24680514]

(19). He N, Yi D, and Fessner WD (2011) Flexibility of Substrate Binding of Cytosine-5′-Monophosphate-N-Acetylneuraminate Synthetase (CMP-Sialate Synthetase) from Neisseria meningitidis: An Enabling Catalyst for the Synthesis of Neo-sialoconjugates. Adv. Synth. Catal 353, 2384–2398.

(20). Yu H, Cao H, Tiwari VK, Li Y, and Chen X (2011) Chemoenzymatic synthesis of C8-modified sialic acids and related α2–3- and α2–6-linked sialosides. Bioorg. Med. Chem. Lett 21, 5037–5040. [PubMed: 21592790]

(21). Mosimann SC, Gilbert M, Dombroswki D, To R, Wakarchuk W, and Strynadka NC (2001) Structure of a sialic acid-activating synthetase, CMP-acylneuraminate synthetase in the presence and absence of CDP. J. Biol. Chem 276, 8190–8196. [PubMed: 11113120]

(22). Krapp S, Munster-Kuhnel AK, Kaiser JT, Huber R, Tiralongo J, Gerardy-Schahn R, and Jacob U (2003) The crystal structure of murine CMP-5-N-acetylneuraminic acid synthetase. J. Mol. Biol 334, 625–637. [PubMed: 14636592]

(23). Heyes DJ, Levy C, Lafite P, Roberts IS, Goldrick M, Stachulski AV, Rossington SB, Stanford D, Rigby SE, Scrutton NS, and Leys D (2009) Structure-based mechanism of CMP-2-keto-3-deoxymanno-octulonic acid synthetase: convergent evolution of a sugar-activating enzyme with DNA/RNA polymerases. J. Biol. Chem 284, 35514–35523. [PubMed: 19815542]

(24). Jelakovic S, and Schulz GE (2001) The structure of CMP:2-keto-3-deoxy-manno-octonic acid synthetase and of its complexes with substrates and substrate analogs. J. Mol. Biol 312, 143–155. [PubMed: 11545592]

(25). Horsfall LE, Nelson A, and Berry A (2010) Identification and characterization of important residues in the catalytic mechanism of CMP-Neu5Ac synthetase from Neisseria meningitidis. FEBS J. 277, 2779–2790. [PubMed: 20491913]

(26). Yi D, He N, Kickstein M, Metzner J, Weiss M, Berry A, and Fessner WD (2013) Engineering of a Cytidine 5′-Monophosphate-Sialic Acid Synthetase for Improved Tolerance to Functional Sialic Acids. Adv. Synth. Catal 355, 3597–3612.

(27). Schmidt H, Mesters JR, Wu J, Woodard RW, Hilgenfeld R, and Mamat U (2011) Evidence for a two-metal-ion mechanism in the cytidyltransferase KdsB, an enzyme involved in lipopolysaccharide biosynthesis. PLoS One 6, e23231. [PubMed: 21826242]

(28). Blacklow RS, and Warren L (1962) Biosynthesis of sialic acids by Neisseria meningitidis. J. Biol. Chem 237, 3520–3526. [PubMed: 13971393]

(29). Andreini C, Cavallaro G, Lorenzini S, and Rosato A (2012) MetalPDB: a database of metal sites in biological macromolecular structures. Nucleic Acids Res. 41, D312–319. [PubMed: 23155064]

(30). Zheng H, Cooper DR, Porebski PJ, Shabalin IG, Handing KB, and Minor W (2017) CheckMyMetal: a macromolecular metal-binding validation tool. Acta Crystallogr. D Struct Biol 73, 223–233. [PubMed: 28291757]

(31). Kabsch W (2010) Xds. Acta Crystallogr., Sect. D: Biol. Crystallogr 66, 125–132. [PubMed: 20124692]

(32). Evans PR, and Murshudov GN (2013) How good are my data and what is the resolution? Acta Crystallogr., Sect. D: Biol. Crystallogr 69, 1204–1214. [PubMed: 23793146]

(33). McCoy AJ, Grosse-Kunstleve RW, Adams PD, Winn MD, Storoni LC, and Read RJ (2007) Phaser crystallographic software. J. Appl. Crystallogr 40, 658–674. [PubMed: 19461840]

(34). Murshudov GN, Skubak P, Lebedev AA, Pannu NS, Steiner RA, Nicholls RA, Winn MD, Long F, and Vagin AA (2011) REFMAC5 for the refinement of macromolecular crystal structures. Acta Crystallogr., Sect. D: Biol. Crystallogr 67, 355–367. [PubMed: 21460454]

(35). Afonine PV, Grosse-Kunstleve RW, Echols N, Headd JJ, Moriarty NW, Mustyakimov M, Terwilliger TC, Urzhumtsev A, Zwart PH, and Adams PD (2012) Towards automated crystallographic structure refinement with phenix.refine. Acta Crystallogr., Sect. D: Biol. Crystallogr 68, 352–367. [PubMed: 22505256]

(36). Munster AK, Weinhold B, Gotza B, Muhlenhoff M, Frosch M, and Gerardy-Schahn R (2002) Nuclear localization signal of murine CMP-Neu5Ac synthetase includes residues required for both nuclear targeting and enzymatic activity. J. Biol. Chem 277, 19688–19696. [PubMed: 11893746]

(37). Schauer R, Haverkamp J, and Ehrlich K (1980) Isolation and characterization of acylneuraminate cytidylyltransferase from frog liver. Hoppe-Seyler's Z. Physiol. Chem 361, 641–648. [PubMed: 6253375]

(38). Bravo IG, Barrallo S, Ferrero MA, Rodriguez-Aparicio LB, Martinez-Blanco H, and Reglero A (2001) Kinetic properties of the acylneuraminate cytidylyltransferase from Pasteurella haemolytica A2. Biochem. J 358, 585–598. [PubMed: 11577688]

(39). Rodriguez-Aparicio LB, Luengo JM, Gonzalez-Clemente C, and Reglero A (1992) Purification and characterization of the nuclear cytidine 5′-monophosphate N-acetylneuraminic acid synthetase from rat liver. J. Biol. Chem 267, 9257–9263. [PubMed: 1577759]

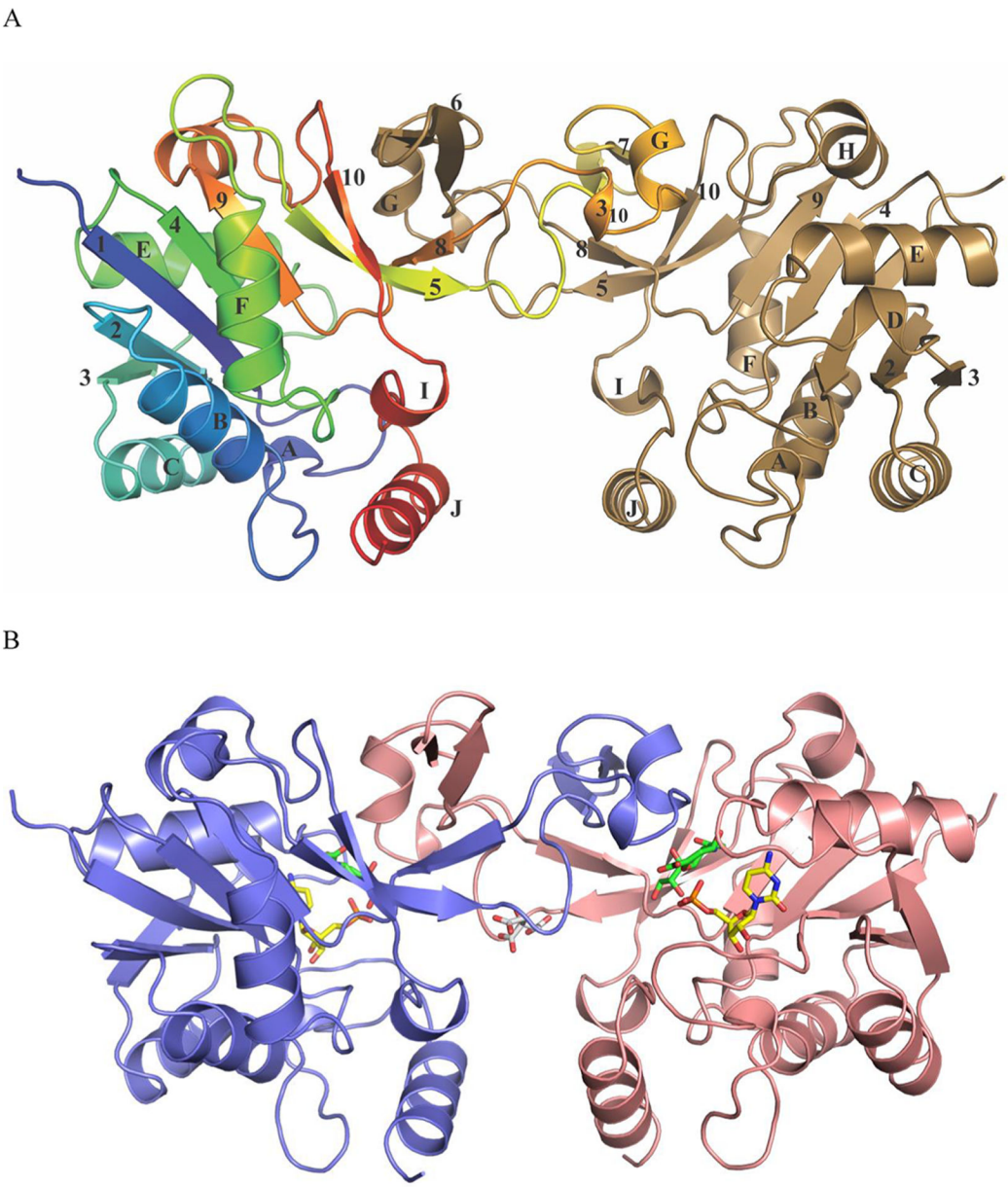


**Figure 1.**

NmCSS homodimer structure. (A) Structure of the ligand-free NmCSS homodimer. For contrast, one monomer is shown in bronze and the other in the rainbow spectrum starting with blue at the N-terminus and ending with red at the C-terminus. Each monomer consists of a globular nucleotide-binding domain and an extended dimerization domain where it interacts with its partner monomer. $\beta$-Sheets are labeled with numbers and $\alpha$-helices with letters, with the exception of the $3_{10}$ helix located in the dimerization domain of each monomer. (B) Structure of NmCSS homodimer with ligands CMP and Neu5Ac2en bound in the active site, drawn as sticks with yellow- and green-colored carbon atoms, respectively. Citrate binding at dimer interface is drawn in sticks with white-colored carbon atoms.

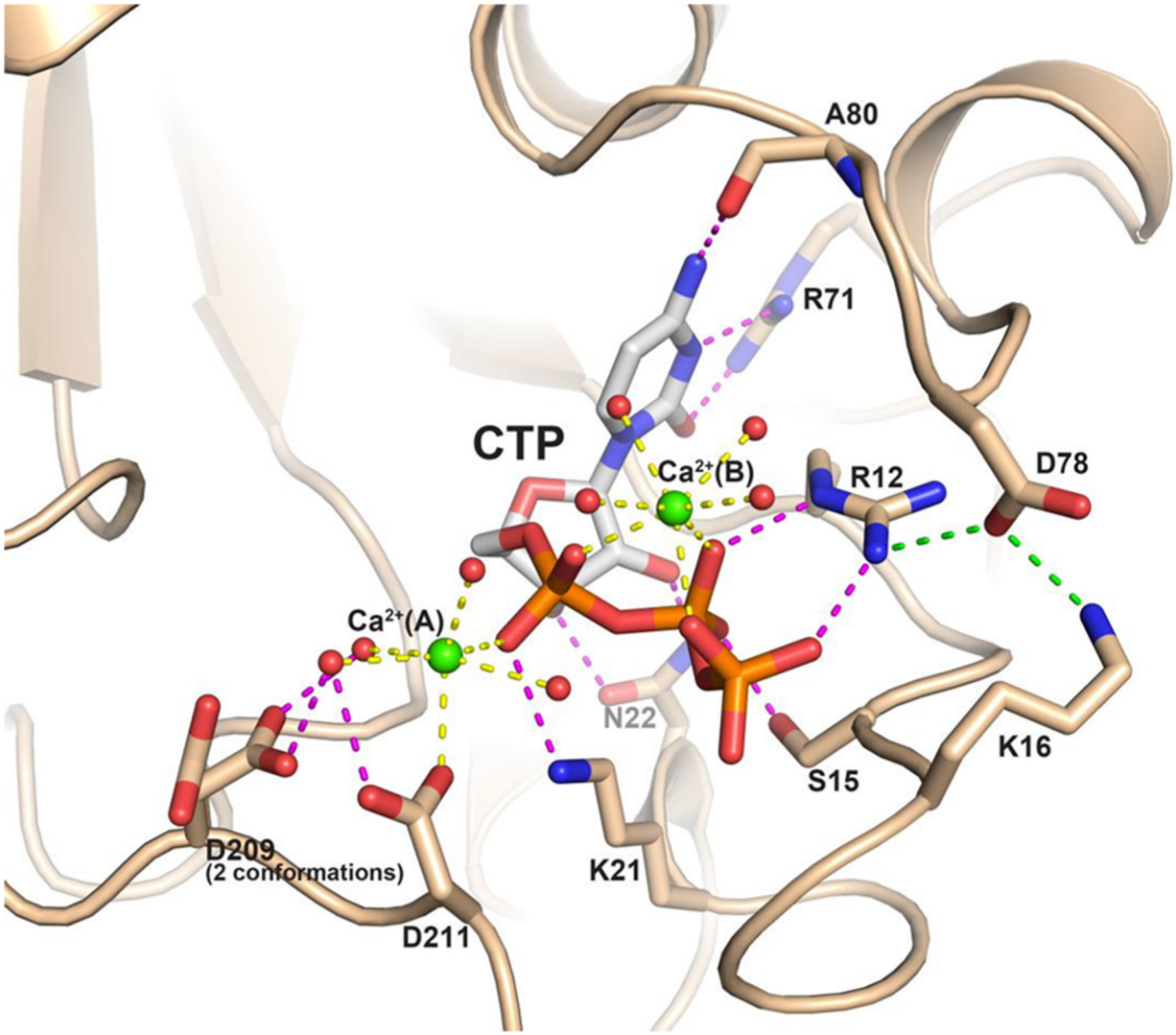


**Figure 2.**

Binding orientation of CTP in the active site. CTP (white carbons) bound in the A subunit of the dimer with two calcium ions (green spheres) ligated to the phosphate moieties. Calcium ions (A and B) work together with the P-loop (residues 12–22) to properly position and stabilize the negative charge on the triphosphate group. Calcium ion A ligates to the $\alpha$-phosphate, Asp211, and four water molecules (red spheres). Asp209, which was observed to adopt two conformations with one binding to the $Ca^{2+}$(A) water ligands, together with Asp211 make up the conserved DXD motif. Calcium ion B ligates to all three phosphates of CTP together with four water molecules. Calcium ligations are highlighted with yellow dashed lines, and hydrogen bonds between the protein and Ca-CTP are magenta in color, while the P-loop stabilization interaction between Arg12-Asp78-Lys16 is drawn with green dashed lines.

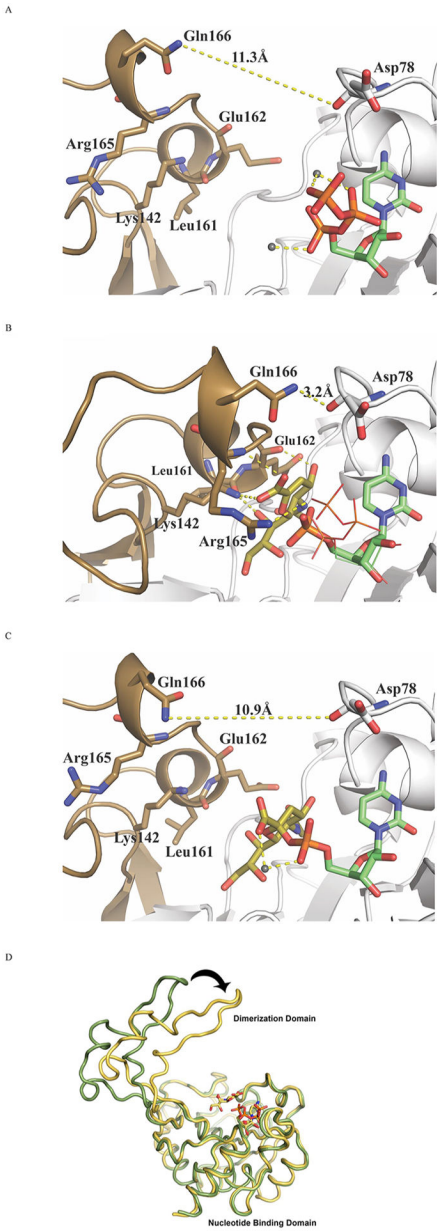


**Figure 3.**

Mechanism of active site closing. (A) After CTP and $Ca^{2+}$ bind to monomer A, the enzyme maintains in the open state until the arrival of sialic acid. (B) As Neu5Ac2en binds to the nucleotide-binding (NB) domain of monomer A (white), interactions involving 5 residues from the dimerization domain of monomer B (brown) and sialic acid (yellow sticks) cause the distance between dimerization and NB domain to decrease by up to 8 Å. (C) After formation of product, contacts between the dimerization domain and sialic acid are broken, and the active site is reopened. (D) Superposition of nucleotide-binding domains of the A monomers from the CTP-bound structure (green) onto the CMP/Neu5Ac2en structure (yellow). Relative orientation of the dimerization domain rotates closed upon binding Neu5Ac2en (highlighted by arrow).

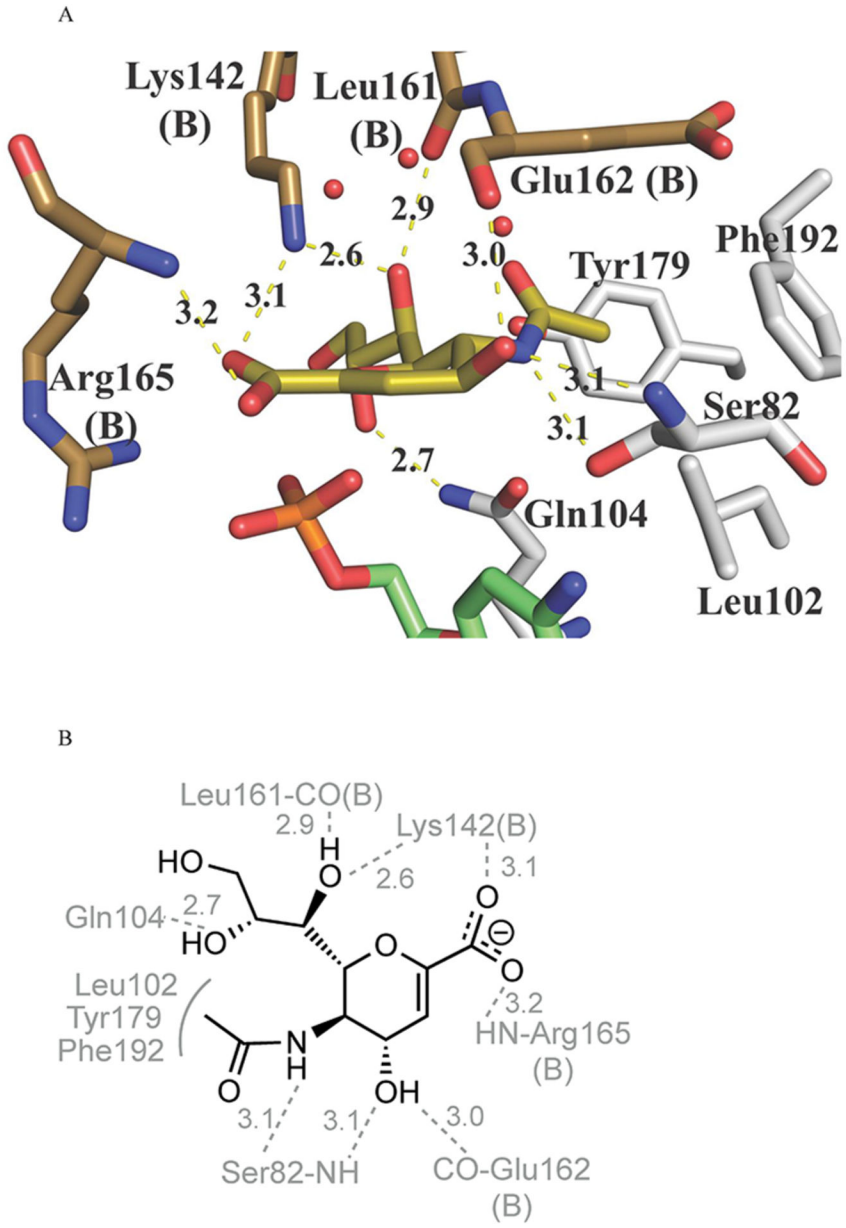


**Figure 4.**

Ligands involved in dimer closing. (A) The sialic acid analogue (yellow) has numerous contacts with both the nucleotide-binding domain of monomer A (white sticks) and the dimerization domain of monomer B (brown sticks). Three ordered water molecules indicate a solvent pocket, which may allow for substrate variation. (B) Summary of contacts between NmCSS and Neu5Ac2en.

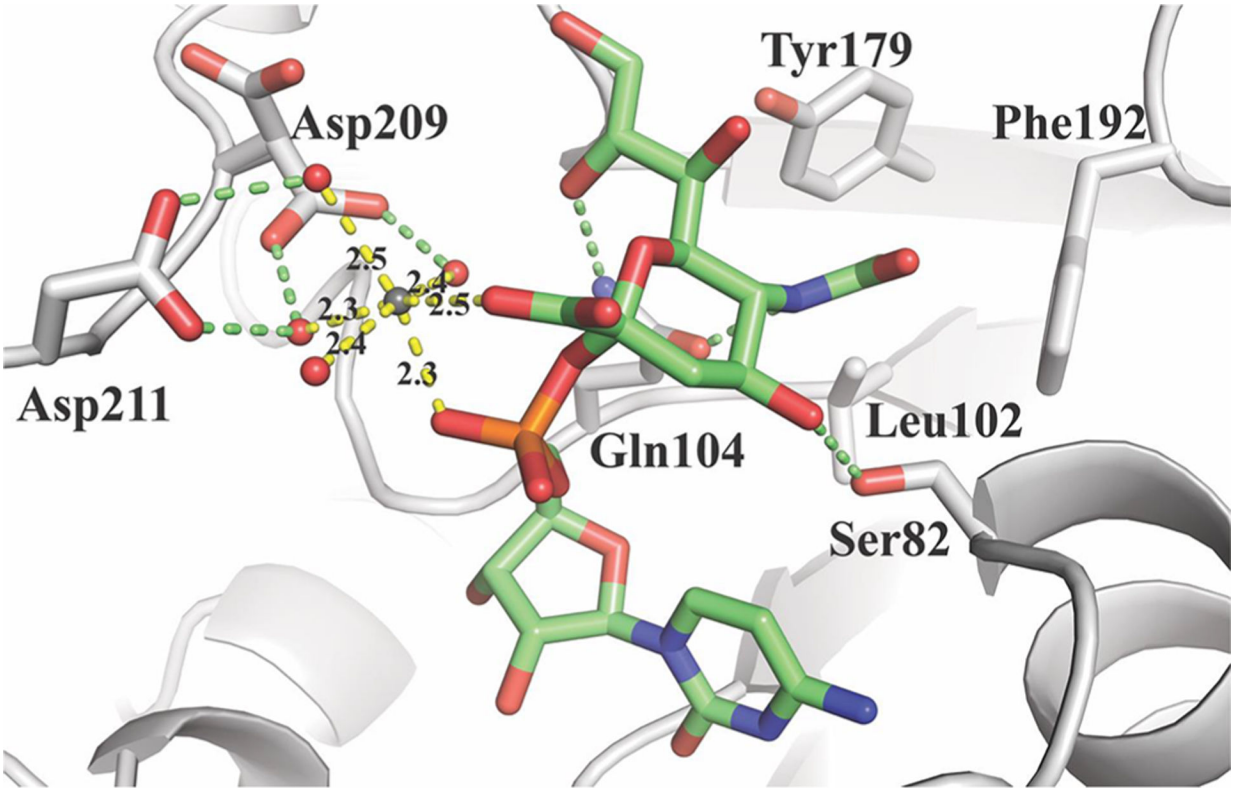


**Figure 5.**

Product-bound open state of the NmCSS active site. After CMP-Neu5Ac product formation (green-colored bonds), the enzyme releases pyrophosphate and $Ca^{2+}$(B) and leaves behind $Ca^{2+}$(A) and product. Interactions between sialic acid and the nucleotide-binding domain are maintained, but those between sialic acid and the dimerization domain of the opposite monomer are broken.

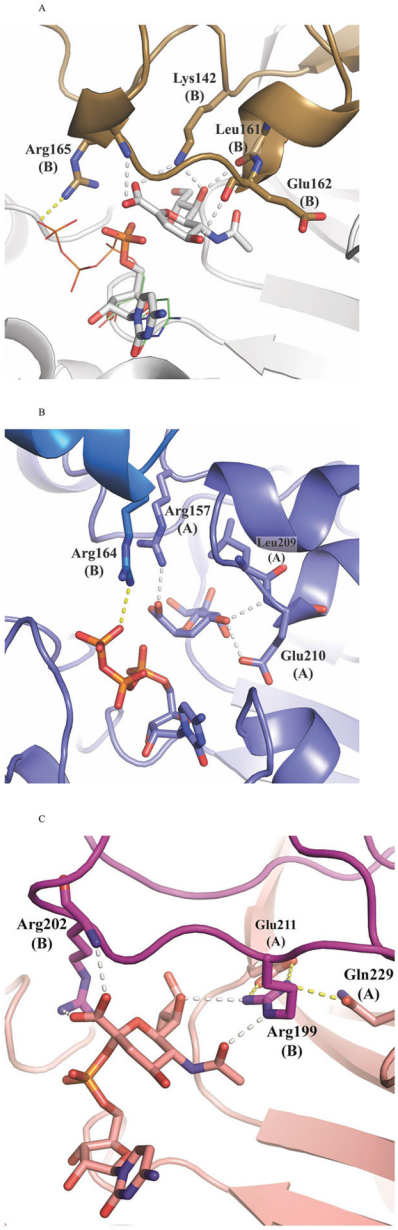


**Figure 6.**

Comparison of NmCSS to similar enzymes. Interactions between protein and sugar are white dashes. Those between protein and nucleotide are yellow. (A) NmCSS/CMP/Neu5Ac2en with an overlay of CTP (sticks) from the NmCSS/CTP structure, highlighting residues from an opposite monomer, which interact with sialic acid and possibly with CTP. Panels B and C focus on only a small selection of relevant protein–sugar interactions for comparison to Lys142 and Arg165 of NmCSS. (B) EcKdsB/CTP/Kdo2en (PDB ID 3K8D). Kdo2en is a nonreacting analogue of KdsB's natural substrate. (C) MmCSS/CMP-Neu5Ac (PDB ID 1QWJ). A bridging arginine between the dimerization domain and substrate of the opposite monomer is a common feature.

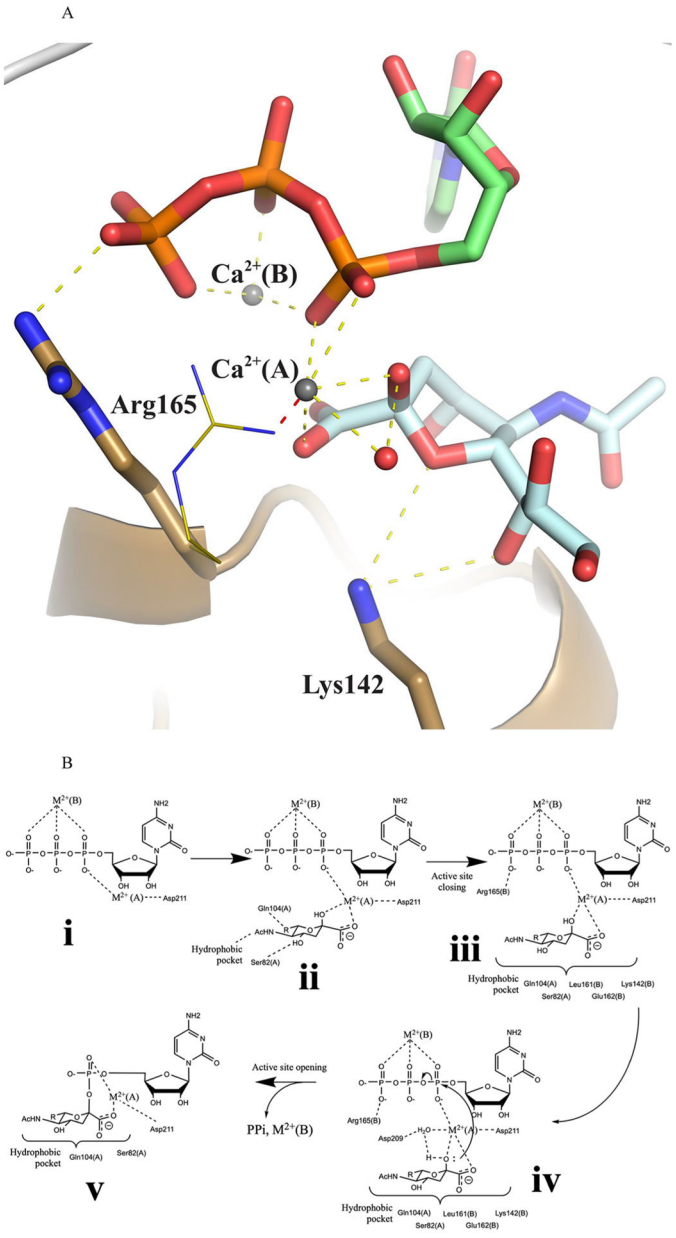


**Figure 7.**

Proposed mechanism of NmCSS. (A) Model of the NmCSS active site in the presence of both substrates. The conformation of CTP (green sticks) in the presence of $Ca^{2+}$(A) and $Ca^{2+}$(B) (gray spheres) superimposed into the NmCSS/CMP/Neu5Ac2en active site, in which Neu5Ac2en has been replaced with Neu5Ac suggests a clash (red dashes) between $Ca^{2+}$(A) and Arg165 (thin brown sticks). However, a different rotamer of Arg165 (thick brown sticks) would allow for the observed $Ca^{2+}$(A) placement while preserving the negative-charge stabilization of CTP's $\gamma$-phosphate by the arginine guanidinium group. (B) (i) CTP binds to the nucleotide binding (NB) domain first in addition to two divalent cations. (ii) Next, Neu5Ac enters the active site and associates initially with the NB domain but quickly (iii) draws together the NB and dimerization domains to form the closed state (all

residues involved in Neu5Ac binding are summarized below the structure for simplicity. (iv) Divalent cation $M^{2+}$ coordinates the C2-OH, allowing a water molecule to deprotonate C2-OH long enough for the hydroxyl O to attack the $\alpha$-phosphate. (v) After product formation, pyrophosphate ($PP_i$) and $M^{2+}$(B) are released from the active site and the active site reopens.

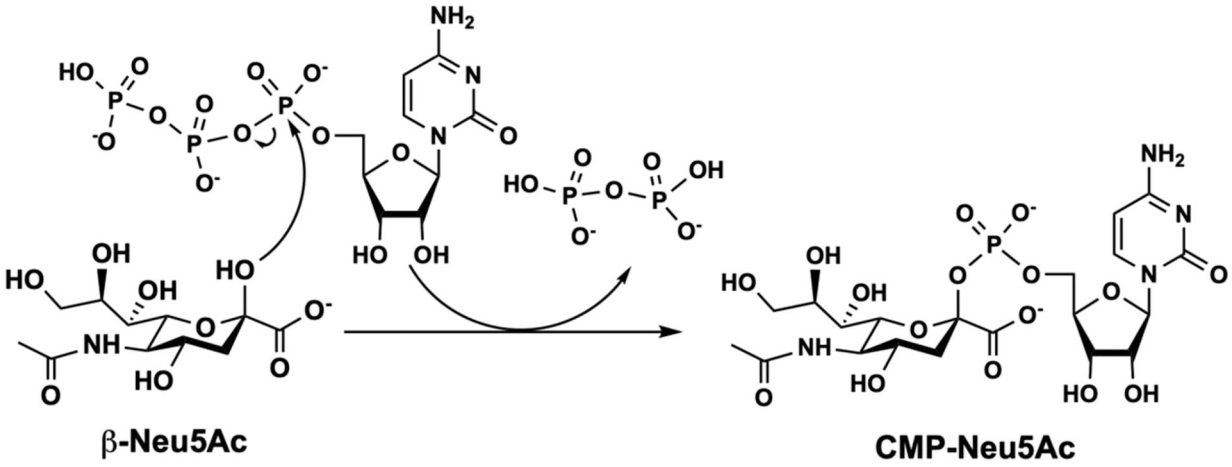


**Scheme 1.**
Reaction Catalyzed by CMP-Sialic Acid Synthetases (CSSs)

*Biochemistry*. Author manuscript; available in PMC 2021 January 19.

**Table 1.**

Data Processing and Refinement Statistics

| **complex** | **CSS** | **CSS/CTP/Ca/Ca** | **CSS/CMP/Neu5Ac2en** | **CSS/CMP-Neu5Ac/Ca** |
|---|---|---|---|---|
| PDB ID | 6CKJ | 6CKK | 6CKL | 6CKM |
| beamline | APS 24-ID-C | SSRL 7–1 | SSRL 7–1 | SSRL 7–1 |
| wavelength (Å) | 0.9791 | 1.03316 | 0.97950 | 1.12709 |
| space group | C222 | $P2_12_12_1$ | $C222_1$ | C222 |
| unit cell parameters (Å) | $a$ = 93.78, $b$ = 155.06, $c$ = 38.78 | $a$ = 43.19, $b$ = 69.56, $c$ = 158.21 | $a$ = 128.48, $b$ = 151.01, $c$ = 84.90 | $a$ = 93.37, $b$ = 156.02, $c$ = 38.71 |
| resolution range (Å) | 38.78–1.75 (1.78–1.75) | 37.91–1.80 (1.84–1.80) | 97.86–2.68 (2.75–2.68) | 80.13–1.54 (1.58–1.54) |
| no. observed reflections | 95 613 (4830) | 142 810 (9562) | 71 705 (4482) | 145 811 (9292) |
| no. unique reflections | 27 855 (1446) | 42 666 (2883) | 22 814 (1615) | 41 624 (2739) |
| completeness (%) | 96.0 (91.8) | 93.8 (87.7) | 97.1 (94.2) | 98.6 (89.4) |
| $I/\sigma(I)$ | 14.2 (3.9) | 16.64 (3.56) | 11.57 (2.13) | 11.86 (2.52) |
| $R_{merge}$[a] (%) | 6.2 (51.5) | 4.8 (29.1) | 8.9 (50.3) | 6.1 (44.9) |
| $CC_{1/2}$ | 99.5 (79.4) | 99.8 (92.0) | 99.5 (72.7) | 99.7 (79.8) |
| monomers per ASU | 1 | 2 | 3 | 1 |
| Matthew's coefficient (Å$^3$/Da) | 2.75 | 2.32 | 2.68 | 2.75 |
| solvent content (%) | 55.27 | 46.93 | 54.06 | 55.28 |
| | | Refinement Statistics | | |
| no. of reflections ($F > 0$) | 27 840 | 40 429 | 21 689 | 41 623 |
| $R_{factor}$[b] (%) | 15.71 | 20.19 | 19.44 | 15.28 |
| $R_{free}$[b] (%) | 18.65 | 24.96 | 24.17 | 17.63 |
| RMS bond length (Å) | 0.006 | 0.016 | 0.012 | 0.006 |
| RMS bond angle (deg) | 0.751 | 1.728 | 1.598 | 0.763 |
| coordinate error (Å) | 0.13 | 0.11 | 0.25 | 0.14 |
| | | Ramachandran Plot Statistics[c] | | |
| favored (%) | 98.21 | 97.09 | 98.06 | 98.65 |
| allowed (%) | 1.79 | 2.69 | 1.49 | 1.35 |
| outliers (%) | 0.00 | 0.22 | 0.45 | 0.00 |
| | | No. of Atoms (B-Factor) | | |

| complex | CSS | CSS/CTP/Ca/Ca | CSS/CMP/Neu5Ac2en | CSS/CMP-Neu5Ac/Ca |
|---|---|---|---|---|
| protein | 1719 (27.40) | 3497 (21.61) | 5174 (44.04) | 1721 (23.49) |
| ligand | 0 | 58 (20.88) | 123 (37.68) | 41 (25.49) |
| metal | 2 (37.48) | 3 (30.45) | 0 | 1 (35.30) |
| solvent | 256 (35.96) | 680 (33.02) | 140 (38.05) | 309 (35.75) |

[a] $R_{merge} = [\Sigma_h\Sigma_i|I_h - I_{hi}|/\Sigma_h\Sigma_i I_{hi}]$ where $I_h$ is the mean of $I_{hi}$ observations of reflection *h*. Numbers in parentheses represent highest resolution shell.

[b] *R*-Factor and $R_{free} = \Sigma||F_{obs}| - |F_{calc}||/\Sigma|F_{obs}| \times 100$ for 95% of recorded data (*R*-factor) or 5% data ($R_{free}$).

[c] Ramachandran plot statistics from MolProbity.

*Biochemistry*. Author manuscript; available in PMC 2021 January 19.

**Table 2.**

Relative Specific Activity of NmCSS Mutants Compared to the Wild-Type NmCSS

| NmCSS | relative specific activity |
|---|---|
| wild-type | 1.00 ± 0.04 |
| E162A | $(1.45 \pm 0.11) \times 10^{-1}$ |
| E162Q | $(1.53 \pm 0.04) \times 10^{-1}$ |
| R165A | $(1.63 \pm 0.09) \times 10^{-3}$ |